Multi-dimensional oscillatory activity of mouse GnRH neurons in vivo

Su Young Han[1], Shel-Hwa Yeo[1], Jae-Chang Kim[2], Ziyue Zhou[1] and Allan E. Herbison[1]

[1]Department of Physiology, Development and Neuroscience, Downing site, University of Cambridge, Cambridge CB2 3EG, UK and [2]Zurich Center for Neuroeconomics, Department of Economics, University of Zurich, 8006 Zurich, Switzerland

Corresponding author: Prof. Allan Herbison aeh36@cam.ac.uk

Disclosures: The authors have nothing to disclose and no competing interests.

Abstract

The gonadotropin-releasing hormone (GnRH) neurons represent the key output cells of the neural network controlling mammalian fertility. We used GCaMP fiber photometry to record the population activity of the GnRH neuron distal projections in the ventral arcuate nucleus where they merge before entering the median eminence to release GnRH into the portal vasculature. Recordings in freely behaving intact male and female mice revealed abrupt ~8-min duration increases in activity that correlated perfectly with the appearance of a subsequent pulse of luteinizing hormone (LH). The GnRH neuron dendrons also exhibited a low level of unchanging clustered, rapidly fluctuating baseline activity in males and throughout the estrous cycle in females. In female mice, a gradual increase in basal activity that exhibited ~80-min oscillations began in the afternoon of proestrus and lasted for 12 h. This was associated with the onset of the LH surge that ended several hours before the fall in GCaMP signal. Abrupt 8-min duration episodes of GCaMP activity continued to occur on top of the rising surge baseline before ceasing in estrus. These observations provide the first description of GnRH neuron activity in freely behaving animals. They demonstrate that three distinct patterns of oscillatory activity occur in GnRH neurons. These are comprised of low-level rapid baseline activity, abrupt 8-min duration oscillations that drive pulsatile gonadotropin secretion and, in females, a gradual and very prolonged oscillating increase in activity responsible for the preovulatory LH surge.

Introduction

The founding concepts of reproductive neuroendocrinology arose from the recognition by Harris and colleagues of the neurohumoral basis of the hypophyseal pituitary system (Harris 1955, Fink 2015) and the subsequent discovery by Schally and Guillemin and co-workers of the decapeptide gonadotropin-releasing hormone (GnRH) (Amoss, Burges et al. 1971, Schally, Arimura et al. 1971). This was soon followed by an appreciation that GnRH neurons had a very unusual topography in which cell bodies scattered throughout the basal forebrain sent projections to converge on the median eminence to release GnRH into the portal system (Barry 1979). The quest to understand the patterns of GnRH released into the portal system were largely solved by the portal bleeding approach in sheep (Clarke and Cummins 1982, Caraty and Locatelli 1988). Notably, this revealed that abrupt increments of GnRH secretion evoked pulsatile gonadotropin secretion whereas, in females, prolonged increases in constant or episodic GnRH secretion were responsible the preovulatory luteinizing hormone (LH) surge (Karsch, Bowen et al. 1997, Clarke 2018).

Establishing the activity patterns of GnRH neurons *in vivo* has been hampered considerably by their widely dispersed topography and, five decades on, remains an elusive goal (Herbison 2015, Constantin 2017). The development of transgenic GnRH-GFP mouse lines greatly facilitated efforts to record the electrical properties of individual GnRH neurons in the acute brain slice (Constantin, Moenter et al. 2021). However, the patterns of firing exhibited by GnRH neurons under these conditions do not align well with predicted pulse or surge patterns of GnRH secretion (Herbison 2015, Constantin, Moenter et al. 2021). Similarly, the only report of GnRH neuron firing *in vivo* to date described a range of irregular firing patterns inconsistent with known hormone secretion (Constantin, Iremonger et al. 2013).

The episodic pattern of GnRH secretion driving pulsatile LH release is generated by the intermittent synchronised activity of the arcuate kisspeptin neuron population that projects to and controls the distal processes of GnRH neurons (Herbison 2018, Goodman, Herbison et al. 2022). These processes, termed dendrons in rodents, converge in the ventrolateral aspects of the arcuate nucleus (ARN) before turning into short axons that run into the median eminence (Herbison 2021). The GnRH neuron dendron appears to operate as an autonomous site for GnRH pulse secretion whilst also carrying action potentials driving the GnRH surge that are initiated upstream at the level of the GnRH neuron cell bodies (Herbison 2020).

We have previously documented that the expression of GCaMP in GnRH neuron cell bodies and dendrons can be used to faithfully record GnRH neuron electrical activity *in vitro* (Iremonger, Porteous et al. 2017). As the ventrolateral ARN provides a unique location of concentrated GnRH neuron dendrons, we reasoned that it may be possible to record their activity in freely behaving mice at this location using GCaMP fiber photometry. We now demonstrate that this is indeed

possible and describe here the patterns of GnRH neuron activity underlying episodic and surge patterns of hormone secretion in male and female mice.

Results

Characterization of Gnrh1-GCaMP mouse

The Gnrh1-Cre mouse line (JAX stock #021207) (Yoon, Enquist et al. 2005) was crossed with the Ai162 (TIT2L-GC6s-ICL-tTA2)-D Cre-dependent GCaMP6s line (JAX stock #031562) (Daigle, Madisen et al. 2018) to generate Gnrh1-GCaMP6 mice. Dual immunofluorescence in four female mice demonstrated that 90±2% of GnRH neuron cell bodies expressed GCaMP within the rostral preoptic area (Fig.1A) as did the majority of GnRH dendrons and fibers within the ME (Fig.1B). In successfully recorded mice, optic fibers were found to be located immediately above or within the mid-caudal ARN (Fig.1C). Mice with unsuccessful recordings (n=4), that displayed no variation in GCaMP signal over 24h recordings, were found to have optic fibers located either mostly within the third ventricle or >200μM lateral to the ARN.

GnRH neuron activity in male mice

The GnRH neuron population activity at the level of distal dendron was measured for 24h starting between 10.00-11.00am in freely behaving Gnrh1-GCaMP6 male mice (n=7). Mice exhibited intermittent, abrupt increases in GCaMP signal termed here “dendron-synchronization episodes” (dSEs; Fig.2A). These episodes had a total duration of ~10 min (658±5s) comprised of a rapid increase (full width at half maximum (FWHM) value of 30±4 s) and a slower decline (FWHM 102±7 s) (Fig.2C). The dSEs occurred on average every 93.3±7.4 min but had a large inter-interval range of 3.9 to 346.6 min. The inter-peak interval distribution was right-skewed (Skewness = 1.39, W = 0.87, P<0.0001, Shapiro-Wilk test) and showed no clear modal pattern (Kurtosis = 1.81, indicating that the data is more spread out than a normal distribution which has a kurtosis of 3.0; Fig.2D). The 24-h recordings also revealed a low amplitude, higher frequency baseline pattern activity (Fig.2A). Control recordings from mice with misplacement of fibers exhibited almost no baseline activity (Fig.2B).

The characteristics of dSEs strongly resembled those exhibited by arcuate nucleus kisspeptin neurons that drive pulsatile luteinizing hormone (LH) secretion (Han et al., 2019). Therefore, we assessed the relationship of GnRH neuron dSEs to LH pulses by taking 5- to 10-minute tail-tip blood samples for up to 240-min period while monitoring GCaMP fluorescence. This showed a perfect association between dSE occurrence and LH pulses (Fig.2E). Analysis of the temporal relationship between dSEs and LH pulses revealed that the peak of dSE consistently preceded LH pulses by 5.0±0.9 min (N=6 episodes in 5 mice; Fig.2F).

GnRH neuron activity in female mice

To examine patterns of GnRH neuron activity across the estrous cycle, female Gnrh1-GCaMP6 mice were recorded for 6 h periods between 10am-4pm on each day of the cycle determined by vaginal cytology on the morning of the recording. Similar to males, freely behaving female mice exhibited a variable baseline pattern of high-frequency activity upon which intermittent, abrupt increases in GCaMP signal occurred (Fig.3A). Each dSE had a total duration of ~ 8 min (463±22s) with a rapid increase (FWHM 31±3 s) and a slower decline (FWHM 81±6 s) (Fig.3B). The frequency of dSEs varied across the cycle in the same manner as kisspeptin neuron SEs (McQuillan, Han et al. 2019) with a dramatic slowing during estrus (dSE interval of 151.0±35.3 min; P=0.01 vs diestrus and 0.001 vs proestrus, Dunn's posthoc; n=5) (Fig.3C). The inter-dSE intervals for metestrus, diestrus and proestrus were not significantly different with mean±SEM of 70.2±6.7 min (n=8), 46.2±4.2 min (n=8), and 38.8±3.4 min (n=6), respectively (Fig.3C). The pattern of the inter-peak interval distribution of dSEs interval was determined in each estrous cycle. In all cycles, the distribution pattern failed the normality test (metestrus [W=0.92, P=0.0007], diestrus [W=0.88, P<0.0001], proestrus [W=0.92, P=0.0007], estrus [W=0.94, P=0.03], Shapiro-Wilk test). In metestrus, diestrus and proestrus, the distribution was right-skewed (skewness= 0.83, 1.37 and 1.13, respectively) with diestrus showing the most pronounced skew (Fig.3.Aii). In metestrus, most dSEs occurred within an interval range of 46-55 minutes (17.5%), while in diestrus and proestrus, the most frequent range was 16-25 min (26.0% and 25.0%, respectively)(Fig.3A). In contrast, during estrus, the inter-peak distribution patten was nearly symmetric (skewness = 0.59) with a flatter and broad shape, showing no clear modal distribution (kurtosis=-0.41) (Fig.3D). The kurtosis values were -0.22, 2.01, 1.84, and -0.41 in metestrus, diestrus, proestrus and estrus, respectively. A kurtosis of 3.0 indicates normally distributed data, suggesting that the inter-peak intervals in diestrus and proestrus have a moderate peak, while the negative kurtosis values of estrus in particular indicate a flatter and broader distribution.

To examine the relationship of dSEs to LH pulses, tail-tip blood sampling was performed and dSEs were found to have a perfect correlation with LH pulses wherein the peak of a dSE occurred 6.1±0.2 min (N=6 episodes in 4 mice) before the peak of the following LH pulse (Fig.3E,F).

Low amplitude, clustered baseline activity in GnRH neurons in both male and female mice

A low-amplitude, high-frequency GCaMP signal was observed in both male and female mice (Fig.2A, 3A, 4A,B). This activity occurred in a cluster-like manner with mean cluster durations of

22.5±2.8 min (males), 30.0±3.9 min (metestrus), 31.9±6.7 min (diestrus) 24.8±2.2 min (proestrus) and 35.3±6.8 min (estrus) in female mice. The intra-cluster frequency (range of 0.006-0.018 Hz) was not different between males and females (Fig.4D). Neither the mean duration nor intra-cluster frequency of the baseline activity were different between males and females or across the estrous cycle (Fig.4C,D). The amplitude of baseline signal was 10-12% (males) and 5-12% (females) of the mean amplitude of dSEs.

GnRH neuron activity in proestrous female mice

To examine patterns of GnRH neuron activity at the time of the preovulatory surge, female Gnrh1-GCaMP6 mice (n=7) were recorded for a 24-hour period beginning on the morning of proestrus. Initially, the signals were identical to those observed on metestrus and diestrus with a low level of high-frequency baseline activity upon which abrupt, short increases in activity occurred (Fig.3A,5A). A gradual increase in baseline activity was observed to begin 4.0±0.5 h (range 2-6.5 h) before "lights-off" (19:00h, 12:12 lighting) that peaked 5.9±0.5 h later and declined to baseline by 12.6±0.8 h (range: 10.3-15.0 h)(Fig.5A). The FWHM period of incline and decline of this slow activity was 3.1±0.4 and 4.7±0.5 h respectively. The slow increment in calcium signal was not smooth but consisted of multiple slow oscillations (Fig.5A). The mean duration of these slow oscillations was 78±4 min (range 32 to 150 min). In addition, dSEs were observed to occur superimposed upon the slow oscillating signal until around the time of peak baseline increment at which time they stopped for several hours (Fig5A). Similar duration 24-hour recordings from metestrus-diestrous female mice found only dSEs without any baseline shifts.

To assess the relationship of the slow oscillating signal to the LH surge, tail-tip bleeding with a 3-hour interval was undertaken (Fig.5B). This showed that the LH surge began at the time of baseline GCaMP change and peaked at 9.3±2.8 ng/ml close to when baseline GCaMP level was at its highest ($\Delta F/F$ of 20-40%) (n=4). Notably, GCaMP activity greatly outlasted the duration of the LH surge (Fig.5B).

To clarify the different components of GCaMP activity occurring on proestrus, we used a customized Matlab code to separate out the three signals occurring at this time (Fig.6). Firstly, a 30-min rolling average was used to extract the slow oscillatory rise and decline in GCaMP activity (Fig.6ii). The subtraction of this 'surge signal' from the original signal (Fig.6A) shows the stereotypical dSEs and baseline fluctuations more clearly (Fig.6iii). Next, the peaks of individual dSEs were selected and the signals from 60 s before and 360 s after each peak of dSE were extracted. The remaining signals are considered to be 'the residual signal' comprising the high-frequency basal activity described above (Fig.6iv).

Discussion

We reveal here three distinct oscillatory patterns of GnRH neuron activity in freely behaving male and female mice. This includes a baseline of high-frequency cluster-like activity upon which abrupt 8-min episodes occur in both males and females, and a prolonged, slowly oscillating rise in activity on the evening of proestrus in females. These patterns of GnRH neuron activity are sufficient to explain the pulse and surge patterns of LH secretion in females and pulses in males.

We demonstrate that the GCaMP fiber photometry approach used previously for assessing cell body population activity in this system (Han, Kane et al. 2019, McQuillan, Han et al. 2019) can be adapted to assess activity in neuronal processes. This has been greatly facilitated by the unusual topography of the GnRH neurons that results in the GnRH neuron projections becoming highly concentrated in the ventrolateral ARN before passing into the ME. The dendrons in this area display substantial rises in intracellular calcium in response to propagating action potentials as well as to the local application of kisspeptin (Iremonger, Porteous et al. 2017, Liu, Yeo et al. 2021). The locations of successful optic fibers immediately above and sometimes lateral to the ARN makes it very unlikely that recordings were made of GnRH neuron activity at the level of their terminals within the ME.

The GnRH neuron dendrons exhibited clustered high-frequency (approximately 0.01Hz) baseline activity that did not change in profile across 24h in males or throughout the estrous cycle. This would be predicted to give rise to fluctuating, low-level inter-pulse GnRH secretion perhaps compatible with observations made using high-frequency portal sampling in the ewe (Evans, Dahl et al. 1995). High-frequency dopamine release also occurs within the ME between events determining prolactin secretion (Romano, Guillou et al. 2017). The physiological significance of inter-pulse GnRH release at the gonadotroph is poorly understood (Le Tissier, Campos et al. 2017). While the self-priming action of GnRH at the gonadotroph is well characterized for the surge, it remains unclear if this exists in relation to pulses (Fink 1995). Indeed, optogenetic experiments driving GnRH neuron firing at high-frequency burst-like intervals in ovariectomized mice were not found to generate any appreciable change in LH secretion *in vivo* (Campos and Herbison 2014).

The origin of fluctuating baseline activity in male and female GnRH neuron dendrons is unknown but it is tempting to speculate that it may arise from synchronised episodic activity of the GnRH neurons themselves. Brain slice electrophysiological studies have consistently documented repetitive burst firing in GnRH neuron cell bodies (Herbison 2015, Constantin, Moenter et al. 2021) and similar patterns of activity were observed in GnRH neurons in anesthetized mice (Constantin, Iremonger et al. 2013). However, the clear clustered patterns of this activity recorded at the dendron would require at least some GnRH neurons to synchronize their activity. To date, there has been no evidence for this with dual or multiple recordings of GnRH neuron cell bodies in brain slices failing to show any coordinated activity (Constantin, Jasoni et al. 2012, Chen and Moenter 2023). Hence, it is possible that the rapid high frequency baseline activity is driven by inputs to

GnRH neurons and, in this respect, it is interesting to note that the ARN kisspeptin neuron pulse generator also exhibits variable high-frequency activity between their synchronizations that drive GnRH pulses (Han, Morris et al. 2023).

We find abrupt increases in GnRH neuron activity preceding each LH pulse that rise to a peak in ~30s and then dissipate over the following 8-10 min. This dynamic is very similar to the reported profile of GnRH secretion into the portal circulation of ovariectomised sheep (Moenter, Brand et al. 1992). The abrupt nature of GnRH neuron activation is also paralleled by the profile of ARN kisspeptin neuron activity during each synchronization event that similarly rises to a peak within 25-50s but then only lasts for a further ~ 1 min (Han, Kane et al. 2019, McQuillan, Han et al. 2019). Kisspeptin released from terminals in the ventrolateral ARN operate through volume transmission to rapidly activate and synchronize GnRH neuron dendrons (Iremonger, Porteous et al. 2017, Liu, Yeo et al. 2021). Alongside evidence that pulsatile LH secretion is abolished in the absence of kisspeptin signaling (Liu, Yeo et al. 2021), it is almost certain that the abrupt episodic GnRH neuron activation recorded here arises from up-stream synchronized firing of ARN kisspeptin neurons. What remains curious, however, is that the effects of exogenous kisspeptin on the dendron are typically prolonged lasting for many 10s of minutes *in vitro* (Iremonger, Porteous et al. 2017, Liu, Yeo et al. 2021). This does not appear to be the case *in vivo* where GnRH neuron activity subsides within 10 min and it is possible that the termination of GnRH neuron dendron firing to provide a relatively constrained secretory signal involves other local mechanisms such as nitric oxide signaling (Constantin, Reynolds et al. 2021).

Investigators using a variety of pituitary portal GnRH assays in rodent, sheep and primate models have suggested that GnRH neurons generate the LH surge through either a constant increase in activity or by increasing their normal pulsatile pattern of release (Sarkar, Chiappa et al. 1976, Caraty, Locatelli et al. 1989, Moenter, Brand et al. 1992, Xia, Van Vugt et al. 1992, Clarke 1993, Pau, Berria et al. 1993, Sisk, Richardson et al. 2001). We demonstrate here that, both predictions were correct with GnRH neuron activity changing in a multi-faceted manner comprised of a slowly oscillating baseline increase with superimposed episodic activity. Retrospectively, this is now readily discernable in many of those portal bleeding data (Sarkar, Chiappa et al. 1976, Caraty, Locatelli et al. 1989, Moenter, Brand et al. 1992, Xia, Van Vugt et al. 1992, Clarke 1993, Pau, Berria et al. 1993, Sisk, Richardson et al. 2001). The slow oscillating increase in baseline activity observed here is most probably the key event driving the LH surge. It initiates at the time the LH surge begins and has a duration of approximately 12 hours which is very similar to that of GnRH release in the portal system of rats, sheep, and monkeys (Sarkar, Chiappa et al. 1976, Pau, Berria et al. 1993, Karsch, Bowen et al. 1997). The reason for the extremely prolonged period of GnRH neuron activity and secretion that long outlasts the LH surge remains unknown but could be related to sexual behavior (Pfaff 1973, Skinner and Caraty 2002).

It has been very surprising to find that this gradual increase in activity itself has a slow hourly oscillatory rhythm. While a circadian contribution to the onset of the surge is well established

(Tonsfeldt, Mellon et al. 2022), it had not been appreciated that an ultradian rhythm might also exist. It is very likely that the slow increase in GnRH activity recorded here is driven by the preoptic surge generator (Wang, Guo et al. 2020), and it will be interesting in future studies to establish whether ultradian rhythms exist within this circuitry and what function they may play in surge generation.

The "two compartment model" of GnRH neurons involves independent pulse and surge generators that operate on different parts of the GnRH neuron to bring about pulsatile and surge patterns of gonadotropin secretion (Herbison 2020). We have recently shown that selective suppression of preoptic area kisspeptin expression abolishes the surge generator but has no impact on pulsatile LH secretion (Clarkson, Yip et al. 2023). This model predicts that, on the afternoon of proestrus, the surge generator would operate coincidently with the pulse generator until such time as post-ovulatory progesterone secretion suppresses the pulse generator (Herbison 2020). This is in perfect agreement with our present *in vivo* recordings where we find abrupt episodic pulse activity to continue on top of the rising phase of the baseline increase until the early hours of estrus when it stops. This highly stereotypical pattern of abrupt episodic activity that reduces in frequency across surge onset is clearly observable after deconvolution of the GCaMP signal (Fig.6) and is identical to that of the ARN kisspeptin pulse generator (McQuillan, Han et al. 2019).

An important question is whether pulse generator activity at the time of the surge may contribute to ovulation. While pulse generator events are short in duration, they nevertheless increase the amplitude of total GnRH neuron activity during the rising phase of the surge and presumably also GnRH secretion within the portal system. Mice and sheep with a knockdown of ARN kisspeptin neurons have recently been reported to have reduced LH surge amplitude (Aerts, Griesgraber et al. 2023, Velasco, Franssen et al. 2023) consistent with the concept proposed here that the pulse generator contributes to the LH surge directly through activation of the GnRH neuron dendron. Intriguingly, toxin-induced knockdown of ARN kisspeptin neurons in rats has the opposite effect of increasing LH surge amplitude (Helena, Toporikova et al. 2015, Mittelman-Smith, Krajewski-Hall et al. 2016).

In summary, we provide here the first direct recordings of GnRH neuron activity *in vivo*. These observations demonstrate that alongside a baseline pattern of activity of unknown function, abrupt episodic activity underlies pulse generation whereas a slow and prolonged ultradian oscillation on proestrus is responsible for the preovulatory gonadotropin surge. The neurobiological mechanisms underlying this unexpected pattern of surge activity remain to be discovered.

Materials and Methods

Animals

Male and female 129S6Sv/Ev C57BL/6 *Gnrh1*$^{Cre/+}$mice (Yoon, Enquist et al. 2005) crossed on to the Ai162 (TIT2L-GC6s-ICL-tTA2)-D Cre-dependent GCaMP6s line (JAX stock #031562) (Daigle, Madisen et al. 2018) were group-housed in conventional cages with environmental enrichment under conditions of controlled temperature (22±2^{0}C) and lighting (12-hour light/12-hour dark cycle; lights on at 07:00) with *ad libitum* access to food (RM1-P, SDS, UK) and water. All animal experimental protocols were approved by the University of Cambridge Animal Welfare and Ethics Review Body under UK Home Office license, P174441DE.

Stereotaxic implantation of optic fibers

Adult mice were anaesthetized with 2% isoflurane and placed in a stereotaxic frame under buprenorphine (0.05mg/kg, s.c.) and meloxicam (5 mg/kg, s.c.) analgesia. Dexamethasone (10 mg/kg, s.c.) was used to prevent cranial swelling. A single 400-μm diameter optic fiber (0.48 NA, Doric lenses, QC, Canada) was implanted into the brain with the tip placed immediately above the dorsomedial part of ARN (A-P to bregma, -2.0mm; D-V 5.9mm, M-L ±0.2mm to sagittal sinus). Following one week of surgery, all animals were handled daily and habituated to a photometry recording setup for at least three weeks.

GCaMP6 fiber photometry and blood sampling

Over a period of 4 to 12 weeks after surgery, fiber photometry experiments were undertaken to record GCaMP fluorescence signal in freely behaving mice for 6 or 24 h periods using previously described methodology (Han, Kane et al. 2019, Han, Morris et al. 2023). This included a custom-built photometry system using Doric components (Doric Lenses, QC, Canada) and National Instrument data acquisition board (TX, USA) based on a previous design (Lerner, Shilyansky et al. 2015). Blue (465-490 nm) and violet (405 nm) LED lights were sinusoidally modulated at frequencies of 531 and 211 Hz respectively and were focused onto a single fiber optic connected to the mouse. The light intensity at the tip of the fiber was 30-80 microwatts. Emitted fluorescence signal from the brain was collected via the same fiber, passed through a 500-550 nm emission filter and focused onto a fluorescence detector (Doric, QC, Canada). The emissions were collected at 10 Hz and the two GCaMP6 emissions were recovered by demodulating the 465-490 nm signals (calcium-dependent) and 405 nm (calcium-independent) signals. Signals were either recorded in a continuous mode or a scheduled 5s on/10s off mode.

Analysis was performed in MATLAB with the subtraction of 405 signal from 465-490 signal to extract the calcium-dependent signal followed by an exponential fit algorithm used to correct for baseline shift. The signal was converted to $\Delta F/F$ (%) values using the equation $\Delta F/F=(F_{recorded}-F_{baseline})/ F_{baseline}) \times 100$. The Findpeaks algorithm was used to detect dSEs, and the duration and the time of SE to the half width full maximum was determined. For deconvolution of signals from 24-h proestrus recordings, the movmean algorithm was used to extract 30-min rolling average.

With this approach, slow oscillatory shifts in baseline during the proestrous surge were detected. The onset and offset of the surge signals were determined by the points at which there was a >5% increment in ΔF relative to all previous timepoints, and when the calcium signal returned to 90% of the baseline value, respectively. The highest value observed during the slow oscillatory phase of the surge was determined to be the peak, and FWHM values were determined from the onset, peak and offset values. The time taken between one trough to another in individual oscillations was calculated as the duration of each oscillation. The second phase of the deconvolution detected all dSE signals using 'findpeaks' algorithm and signals between -60 to 360 s around each peak were separated to visualize the remaining low amplitude 'residual' signal. A threshold of 5% above baseline was used to extract the residual signal. Residual signals with peaks occurring > 420s from the preceding peak were considered to represent separate clusters.

To examine the relationship between calcium episodes with LH pulses, freely behaving mice were attached to the fiber photometry system, and 4-μL blood samples were obtained every 5 to 10 minutes from the tail tip over a period of 120 to 240 minutes. To assess the relationship between the long calcium increment during proestrus evening and the LH surge, female mice were attached to the fiber photometry system in the morning of proestrus and blood samples (3-μL) collected every 3 hours for 18 hours until the morning of estrus. Levels of LH were measured by in-house LH ELISA (Steyn, Wan et al. 2013) with an assay sensitivity of 0.04 ng/mL and intra-assay coefficient of variation of 8.2%.

Immunohistochemistry

Adult GnRH-Cre,GCaMP6s mice were given a lethal overdose of pentobarbital (3mg/100μL, i.p.) and perfused transcardially with 4% paraformaldehyde. Brains were processed for dual GFP and GnRH immunofluorescence. For GFP immunostaining, anti-chicken GFP (1:5000, Aves Lab) was used followed by AlexaFluor 488-conjugated goat-anti-chicken (1:1000). For GnRH cell body immunostaining, GA2 guinea pig anti-GnRH antisera (1:3000, gift from G.Anderson, New Zealand) was used in combination with AlexaFluor 647-conjugated goat anti-guinea pig immunoglobulin (1:500, Thermo Fisher Scientific, USA). For GnRH dendron immunostaining, rabbit anti-GnRH (1:20,000, LR1, gift of R.Benoit, Montreal) antisera was used followed by biotinylated goat anti-rabbit immunoglobulin (1:1000, Jackson Immunoresearch) and AlexaFluor 568-conjugated Streptavidin (1:400, Thermo Fisher Scientific, USA). Imaging was performed using a Leica SP8 Laser Scanning Confocal Microscope (Leica Microsystems) at the Cambridge Advanced Imaging Center and analyzed using ImageJ.

Statistical Analysis

All statistical analyses were performed in Prism 10 (GraphPad software Inc.). All values given in this study are mean ± SEM, and significance is defined as P <0.05* or P<0.01**. For inter-peak interval analysis in females across the estrous cycle and the residual cluster activity analysis, Kruskal Wallis ANOVA followed by Dunn's post-hoc tests was used. For inter-peak interval

distribution patterns, Shapiro Wilk normality test was used where W=1 indicates the sample data are normally distributed. P<0.05 indicates that the data does not follow a normal distribution. Significance is defined as P<0.05*, P<0.01**, P<0.001*** and P<0.0001****.

Acknowledgments

This work was supported by the Wellcome Trust (212242/Z/18/Z). JCK received a Doc.Mobility Fellowship (P1ZHP1_184166) from the Swiss National Science Foundataion. We thank Ms. Maria Pardo-Navarro for technical assistance. For the purpose of open access, the author has applied a Creative Commons Attribution (CC BY) license to any Author Accepted Manuscript version arising from this submission.

Author Contributions: SYH, SHY and ZZ undertook investigations; SYH, SHY and JCK performed analysis; SYH and AEH designed experiments and wrote the manuscript: AEH generated funding.

Figure Legends

Figure 1. *GCaMP expression in GnRH neurons*. (A) Photomicrographs at the level of organum vasculosm of the laminae terminalis (OVLT) showing GFP immunofluorescence representing GCaMP6 (green), GnRH (purple) and merged channels showing double labelled cells (white). (B) Photomicrographs of four mice at the level of arcuate nucleus showing the location of the end of the optic fiber (dotted line) in relation to GnRH neuron dendrons labeled with GnRH (red), GFP representing GCaMP6 (green) and merged channels showing double labelled (yellow). 3V, third ventricle.

Figure 2. *GnRH neuron dendron activity in male mice*. (A) A representative example of 24-h GCaMP6 photometry recording showing abrupt dendron synchronized episodes (dSEs) occurring on lower amplitude baseline activity in a male mouse. Below, expanded view of the trace indicated by the horizontal line. (B) Example of 8-h GCaMP6 photometry recording in a male mouse with a misplaced fiber optic. All recorded signals are under 3% of baseline. Below, expanded view of the trace indicated by the horizontal line. (C) Average high-resolution profile of an dSE in male mice (N=7 mice) showing a rapid onset followed by a gradual decrease back to baseline. 'a' and 'b' give values at full-width half maximum (FWHM). (D) Inter-peak intervals combined from all recordings (n= 96 dSEs) displayed as a percentage of all intervals occurring in 10-min bins. W=0.87, P<0.0001****, Shapiro Wilk normality test. Skewness = 1.39, Kurtosis=1.81. (E) Representative example showing the relationship of dSEs (black) to pulsatile LH secretion (red). (F) Normalized increase in LH plotted against the dSEs, with the time 0 being the peak of dSE.

Figure 3. *GnRH neuron dendron activity in female mice*. (A) Representative example of 6-h GCaMP6 photometry recording from female mice in (i) metestrus, (ii) diestrus, (iii) proestrus, and (iv) estrus. To the right of each trace are histograms showing the mean inter-peak intervals for

dSEs from all recordings across metestrus (n=53 dSEs), diestrus (n=88 dSEs), proestrus (n=62 dSEs) and estrus (n=42 dSEs) displayed as a percentage of all intervals occurring in 10-min bins. In all cycles, the data failed normality test (metestrus [W=0.92, P=0.0007***], diestrus [W=0.88, P<0.0001****], proestrus [W=0.92, P=0.0007***], estrus [W=0.94, P=0.03], Shapiro-Wilk test). (B) Histograms showing inter-peak intervals of dSEs across the estrous cycle. M = metestrus (N=8), D = diestrus (N=8), P = proestrus (N=6), E = estrus (N=5). *P<0.05, **P<0.01, Kruskal Wallis followed by Dunn's post-hoc test. (C) Average high-resolution profile of dSEs in female mice showing a rapid onset followed by a gradual decrease in the signal. 'a' and 'b' show the values at full-width half maximum (FWHM). (D) A representative example showing the relationship of dSEs (black) to pulsatile LH secretion (red). (E) Normalized increase in LH plotted against all dSEs, with the time 0 being the peak of the dSE.

Figure 4. *Baseline high-frequency cluster activity of GnRH neuron dendrons in male and female mice.* Representative 4-h GCaMP recordings in (A) two male mice and (B) a female mouse across the different stages of the estrous cycle showing high frequency baseline activity and larger increases in calcium activity representing dendron synchronization episodes (dSEs) indicated by red asterisks. The peaks of dSEs reaching >30% dFF were cut off to optimize the display of the low amplitude activities. Histograms showing the duration (C) and the intra-cluster frequency (D) of the baseline activity in male and female mice. No significance was found across the groups. M= metestrus, D = diestrus, P = proestrus, E= estrus.

Figure 5. *Slow oscillating increases in calcium activity on the afternoon of proestrus in female mice*. (A) Examples of 21-h GCaMP recordings from four proestrous female mice. Note the prolonged (>10h) gradual oscillating increase in calcium signal beginning on the afternoon of proestrus. The sharp dSEs continue until approximately the plateau phase of the increased baseline at which time they stop or slow. (B) A representative example showing the relationship of the slow increase in baseline calcium activity (black) with LH surge (red). Note that the rise in LH occurs in alongside the initial rise in calcium activity but returns to baseline several hours before the calcium signal.

Figure 6. *Deconvolution of the GCaMP signal across the proestrous surge reveals multimodal activity patterns of GnRH neuron dendron*. (A-B) Representative examples of 24-h photometry recordings from two female mice starting at proestrus showing (i) the original recording, (ii) 30-min rolling average highlighting the LH surge signal (red), (iii) the LH surge signal subtracted from the original recording, displaying the dSEs (blue), and (iv) the residual baseline signal (pink) after subtracting both the surge and pulse profiles.

References

Aerts, E. G., M. J. Griesgraber, S. L. Shuping, E. C. Bowdridge, S. L. Hardy, R. L. Goodman, C. C. Nestor and S. M. Hileman (2023). "The effect of NK3-Saporin injection within the arcuate nucleus on puberty, the LH surge, and the response to Senktide in female sheep." Biol Reprod.

Amoss, M., R. Burges, R. Blackwell, W. Vale, R. Fellows and R. Guillemin (1971). "Purification, amino acid composition and N-terminus of the hypothalamic luteinizing hormone releasing hormone factor (LRF) of ovine origin." Biochemical Biophysical Research Communication. **44**: 205-210.

Barry, J. (1979). "Immunohistochemistry of luteinizing hormone-releasing hormone-producing neurons of the vertebrates." Int Rev Cytol **60**: 179-221.

Campos, P. and A. E. Herbison (2014). "Optogenetic activation of GnRH neurons reveals minimal requirements for pulsatile luteinizing hormone secretion." Proc Natl Acad Sci U S A **111**(51): 18387-18392.

Caraty, A. and A. Locatelli (1988). "Effect of time after castration on secretion of LHRH and LH in the ram." J Reprod Fertil **82**(1): 263-269.

Caraty, A., A. Locatelli and G. B. Martin (1989). "Biphasic response in the secretion of gonadotrophin-releasing hormone in ovariectomized ewes injected with oestradiol." Journal of Endocrinology **123**: 375-382.

Chen, X. and S. M. Moenter (2023). "Gonadal Feedback Alters the Relationship between Action Potentials and Hormone Release in Gonadotropin-Releasing Hormone Neurons in Male Mice." J Neurosci **43**(40): 6717-6730.

Clarke, I. J. (1993). "Variable patterns of gonadotropin-releasing hormone secretion during the estrogen-induced luteinizing hormone surge in ovariectomized ewes." Endocrinology **133**: 1624-1632.

Clarke, I. J. (2018). Generation of the GnRH surge and LH surge by the positive feedback effect of estrogen. The GnRH neuron and its control. A. E. Herbison and T. M. Plant, John Wiley & Sons**:** 325-356.

Clarke, I. J. and J. T. Cummins (1982). "The temporal relationship between gonadotropin releasing hormone (GnRH) and luteinizing hormone (LH) secretion in ovariectomized ewes." Endocrinology **111**(5): 1737-1739.

Clarkson, J., S. H. Yip, R. Porteous, A. Kauff, A. K. Heather and A. E. Herbison (2023). "CRISPR-Cas9 knockdown of ESR1 in preoptic GABA-kisspeptin neurons suppresses the preovulatory surge and estrous cycles in female mice." Elife **12**.

Constantin, S. (2017). "Progress and Challenges in the Search for the Mechanisms of Pulsatile Gonadotropin-Releasing Hormone Secretion." Front Endocrinol (Lausanne) **8**: 180.

Constantin, S., K. J. Iremonger and A. E. Herbison (2013). "In vivo recordings of GnRH neuron firing reveal heterogeneity and dependence upon GABAA receptor signaling." J Neurosci **33**(22): 9394-9401.

Constantin, S., C. Jasoni, N. Romano, K. Lee and A. E. Herbison (2012). "Understanding calcium homeostasis in postnatal gonadotropin-releasing hormone neurons using cell-specific Pericam transgenics." Cell Calcium **51**(3-4): 267-276.

Constantin, S., S. M. Moenter and R. Piet (2021). "The electrophysiologic properties of gonadotropin-releasing hormone neurons." J Neuroendocrinol: e13073.

Constantin, S., D. Reynolds, A. Oh, K. Pizano and S. Wray (2021). "Nitric oxide resets kisspeptin-excited GnRH neurons via PIP2 replenishment." PNAS **118**: e2012339118.

Daigle, T. L., L. Madisen, T. A. Hage, M. T. Valley, U. Knoblich, R. S. Larsen, M. M. Takeno, L. Huang, H. Gu, R. Larsen, M. Mills, A. Bosma-Moody, L. A. Siverts, M. Walker, L. T. Graybuck, Z. Yao, O. Fong, T. N. Nguyen, E. Garren, G. H. Lenz, M. Chavarha, J. Pendergraft, J. Harrington, K. E. Hirokawa, J. A. Harris, P. R. Nicovich, M. J. McGraw, D. R. Ollerenshaw, K. A. Smith, C. A. Baker, J. T. Ting, S. M. Sunkin, J. Lecoq, M. Z. Lin, E. S. Boyden, G. J. Murphy, N. M. da Costa, J. Waters, L. Li, B. Tasic and H. Zeng (2018). "A Suite of Transgenic Driver and Reporter Mouse Lines with Enhanced Brain-Cell-Type Targeting and Functionality." Cell **174**(2): 465-480 e422.

Evans, N. P., G. E. Dahl, D. Mauger and F. J. Karsch (1995). "Estradiol induces both qualitative and quantitative changes in the pattern of gonadotropin-releasing hormone secretion during the presurge period in the ewe." Endocrinology **136**: 1603-1609.

Fink, G. (1995). "The self-priming effect of LHRH: a unique servomechanism and possible cellular model for memory." Front Neuroendocrinol **16**(2): 183-190.

Fink, G. (2015). "60 YEARS OF NEUROENDOCRINOLOGY: MEMOIR: Harris' neuroendocrine revolution: of portal vessels and self-priming." J Endocrinol **226**(2): T13-24.

Goodman, R. L., A. E. Herbison, M. N. Lehman and V. M. Navarro (2022). "Neuroendocrine control of gonadotropin-releasing hormone: Pulsatile and surge modes of secretion." J Neuroendocrinol **34**(5): e13094.

Han, S. Y., G. Kane, I. Cheong and A. E. Herbison (2019). "Characterization of GnRH Pulse Generator Activity in Male Mice Using GCaMP Fiber Photometry." Endocrinology **160**(3): 557-567.

Han, S. Y., P. G. Morris, J. C. Kim, S. Guru, M. Pardo-Navarro, S. H. Yeo, H. J. McQuillan and A. E. Herbison (2023). "Mechanism of kisspeptin neuron synchronization for pulsatile hormone secretion in male mice." Cell Rep **42**(1): 111914.

Harris, G. W. (1955). Neural control of the pituitary gland. London, Edward Arnold.

Helena, C. V., N. Toporikova, B. Kalil, A. M. Stathopoulos, V. V. Pogrebna, R. O. Carolino, J. A. Anselmo-Franci and R. Bertram (2015). "KNDy Neurons Modulate the Magnitude of the Steroid-Induced Luteinizing Hormone Surges in Ovariectomized Rats." Endocrinology **156**(11): 4200-4213.

Herbison, A. E. (2015). Physiology of the adult GnRH neuronal network. Knobil and Neill's Physiology of Reproduction. T. M. Plant and A. J. Zeleznik, Academic Press. **1:** 399-467.

Herbison, A. E. (2018). "The gonadotropin-releasing hormone pulse generator." Endocrinology **159**(11): 3723-3736.

Herbison, A. E. (2020). "A simple model of estrous cycle negative and positive feedback regulation of GnRH secretion." Front Neuroendocrinol **57**: 100837.

Herbison, A. E. (2021). "The dendron and episodic neuropeptide release." J Neuroendocrinol: e13024.

Iremonger, K. J., R. Porteous and A. E. Herbison (2017). "Spike and neuropeptide-dependent mechanisms control GnRH neuron nerve terminal Ca2+ over diverse time scales." J Neurosci **37**(12): 3342-3351.

Karsch, F. J., J. M. Bowen, A. Caraty, N. P. Evans and S. M. Moenter (1997). "Gonadotropin-releasing hormone requirements for ovulation." Biol Reprod **56**: 303-309.

Le Tissier, P., P. Campos, C. Lafont, N. Romano, D. J. Hodson and P. Mollard (2017). "An updated view of hypothalamic-vascular-pituitary unit function and plasticity." Nat Rev Endocrinol **13**(5): 257-267.

Lerner, T. N., C. Shilyansky, T. J. Davidson, K. E. Evans, K. T. Beier, K. A. Zalocusky, A. K. Crow, R. C. Malenka, L. Luo, R. Tomer and K. Deisseroth (2015). "Intact-Brain Analyses Reveal Distinct Information Carried by SNc Dopamine Subcircuits." Cell **162**(3): 635-647.

Liu, X., S. H. Yeo, H. J. McQuillan, M. K. Herde, S. Hessler, I. Cheong, R. Porteous and A. E. Herbison (2021). "Highly redundant neuropeptide volume co-transmission underlying episodic activation of the GnRH neuron dendron." Elife **10**.

McQuillan, H. J., S. Y. Han, I. Cheong and A. E. Herbison (2019). "GnRH Pulse Generator Activity Across the Estrous Cycle of Female Mice." Endocrinology **160**(6): 1480-1491.

Mittelman-Smith, M. A., S. J. Krajewski-Hall, N. T. McMullen and N. E. Rance (2016). "Ablation of KNDy Neurons Results in Hypogonadotropic Hypogonadism and Amplifies the Steroid-Induced LH Surge in Female Rats." Endocrinology **157**(5): 2015-2027.

Moenter, S. M., R. C. Brand and F. J. Karsch (1992). "Dynamics of gonadotropin-releasing hormone (GnRH) secretion during the GnRH surge: insights into the mechanism of GnRH surge induction." Endocrinology **130**(5): 2978-2984.

Moenter, S. M., R. M. Brand, A. R. Midgley and F. J. Karsch (1992). "Dynamics of gonadotropin-releasing hormone release during a pulse." Endocrinology **130**(1): 503-510.

Pau, K. F., M. Berria, D. L. Hess and H. G. Spies (1993). "Preovulatory gonadotropin-releasing hormone surge in ovarian-intact rhesus macaques." Endocrinology **133**: 1650-1656.

Pfaff, D. W. (1973). "Luteinizing hormone-releasing factor potentiates lordosis behavior in hypophysectomized ovariectomized female rats." Science **182**(117): 1148-1149.

Romano, N., A. Guillou, D. J. Hodson, A. O. Martin and P. Mollard (2017). "Multiple-scale neuroendocrine signals connect brain and pituitary hormone rhythms." Proc Natl Acad Sci U S A **114**(9): 2379-2382.

Sarkar, D. K., S. A. Chiappa, G. Fink and N. M. Sherwood (1976). "Gonadotropin-releasing hormone surge in pro-oestrous rats." Nature **264**: 461-463.

Schally, A. V., A. Arimura, Y. Baba, R. M. Nair, H. Matsuo, T. W. Redding and L. Debeljuk (1971). "Isolation and properties of the FSH and LH-releasing hormone." Biochem Biophys Res Commun **43**(2): 393-399.

Sisk, C. L., H. N. Richardson, P. E. Chappell and J. E. Levine (2001). "In vivo gonadotropin-releasing hormone secretion in female rats during peripubertal development and on proestrus." Endocrinology **142**(7): 2929-2936.

Skinner, D. C. and A. Caraty (2002). "Measurement and possible function of GnRH in cerebrospinal fluid in ewes." Reprod Suppl **59**: 25-39.

Steyn, F. J., Y. Wan, J. Clarkson, J. D. Veldhuis, A. E. Herbison and C. Chen (2013). "Development of a methodology for and assessment of pulsatile luteinizing hormone secretion in juvenile and adult male mice." Endocrinology **154**(12): 4939-4945.

Tonsfeldt, K. J., P. L. Mellon and H. M. Hoffmann (2022). "Circadian Rhythms in the Neuronal Network Timing the Luteinizing Hormone Surge." Endocrinology **163**(2).

Velasco, I., D. Franssen, S. Daza-Duenas, K. Skrapits, S. Takacs, E. Torres, E. Rodriguez-Vazquez, M. Ruiz-Cruz, S. Leon, K. Kukoricza, F. P. Zhang, S. Ruohonen, D. Luque-Cordoba, F. Priego-Capote, F. Gaytan, F. Ruiz-Pino, E. Hrabovszky, M. Poutanen, M. J. Vazquez and M. Tena-Sempere (2023). "Dissecting the KNDy hypothesis: KNDy neuron-derived kisspeptins are

dispensable for puberty but essential for preserved female fertility and gonadotropin pulsatility." Metabolism **144**: 155556.

Wang, L., W. Guo, X. Shen, S. Yeo, H. Long, Z. Wang, Q. Lyu, A. E. Herbison and Y. Kuang (2020). "Different dendritic domains of the GnRH neuron underlie the pulse and surge modes of GnRH secretion in female mice." Elife **9**.

Xia, L., D. Van Vugt, E. J. Alston, J. Luckhaus and M. Ferin (1992). "A surge of gonadotropin-releasing hormone accompanies the estradiol-induced gonadotropin surge in the rhesus monkey." Endocrinology **131**: 2812-2820.

Yoon, H., L. W. Enquist and C. Dulac (2005). "Olfactory inputs to hypothalamic neurons controlling reproduction and fertility." Cell **123**(4): 669-682.

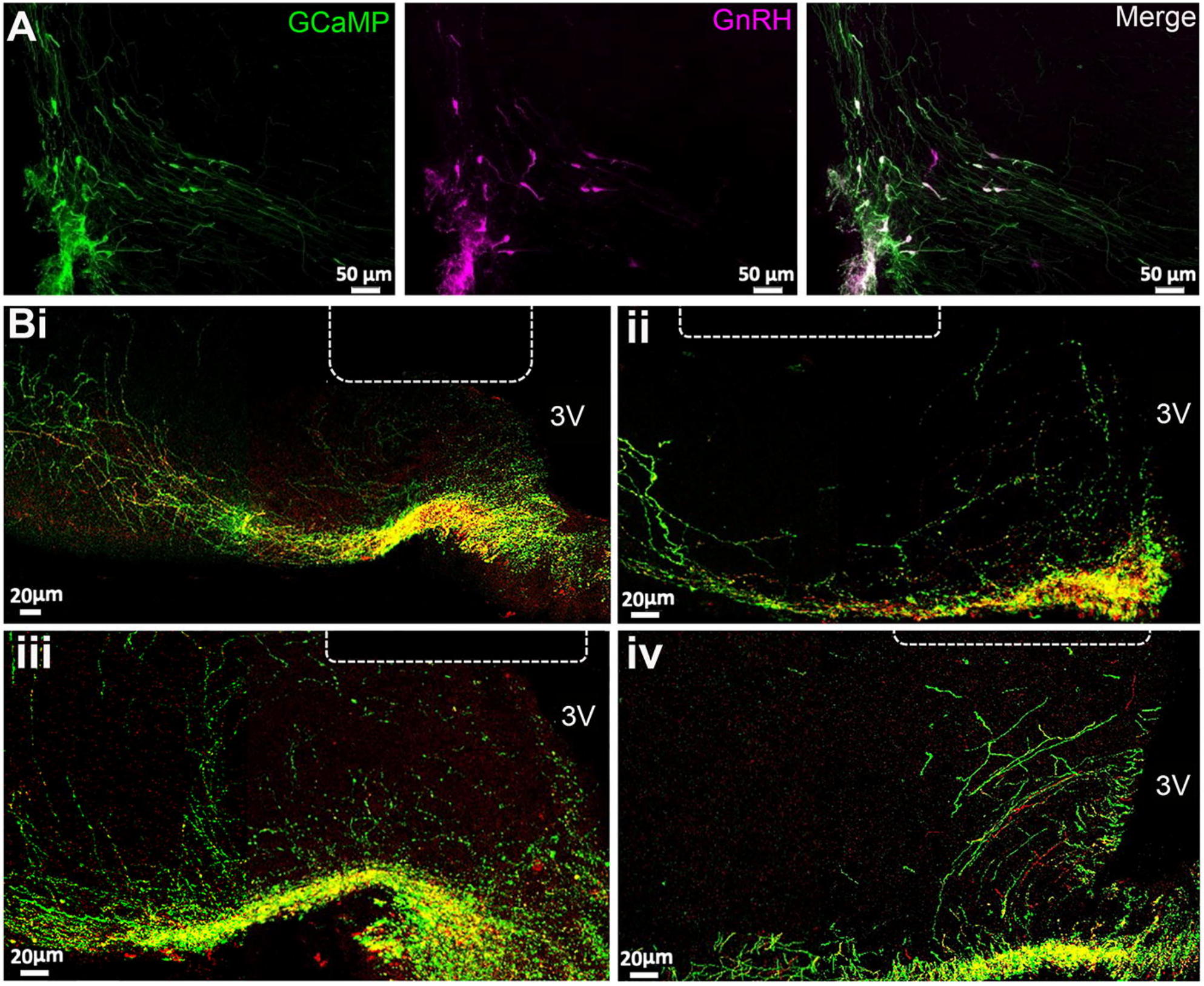
A
GCaMP
50 µm
GnRH
50 µm
Merge
50 µm
Bi
3V
20µm
ii
3V
20µm
iii
3V
20µm
iv
3V
20µm

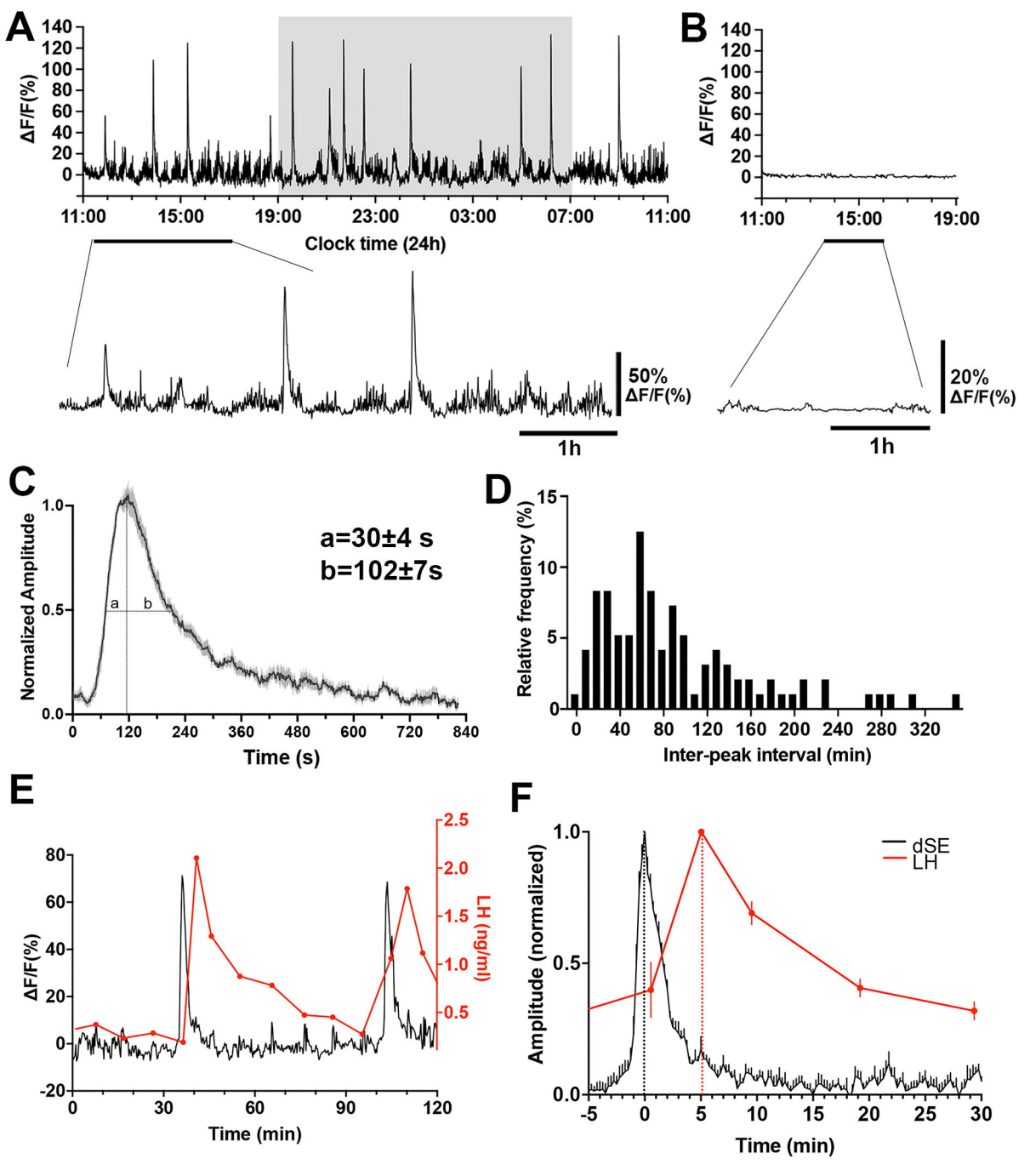
A
ΔF/F(%)
Clock time (24h)
11:00
15:00
19:00
23:00
03:00
07:00
11:00
50% ΔF/F(%)
1h
B
ΔF/F(%)
11:00
15:00
19:00
20% ΔF/F(%)
1h
C
Normalized Amplitude
a=30±4 s
b=102±7s
a
b
Time (s)
D
Relative frequency (%)
Inter-peak interval (min)
E
ΔF/F(%)
LH (ng/ml)
Time (min)
F
dSE
LH
Amplitude (normalized)
Time (min)

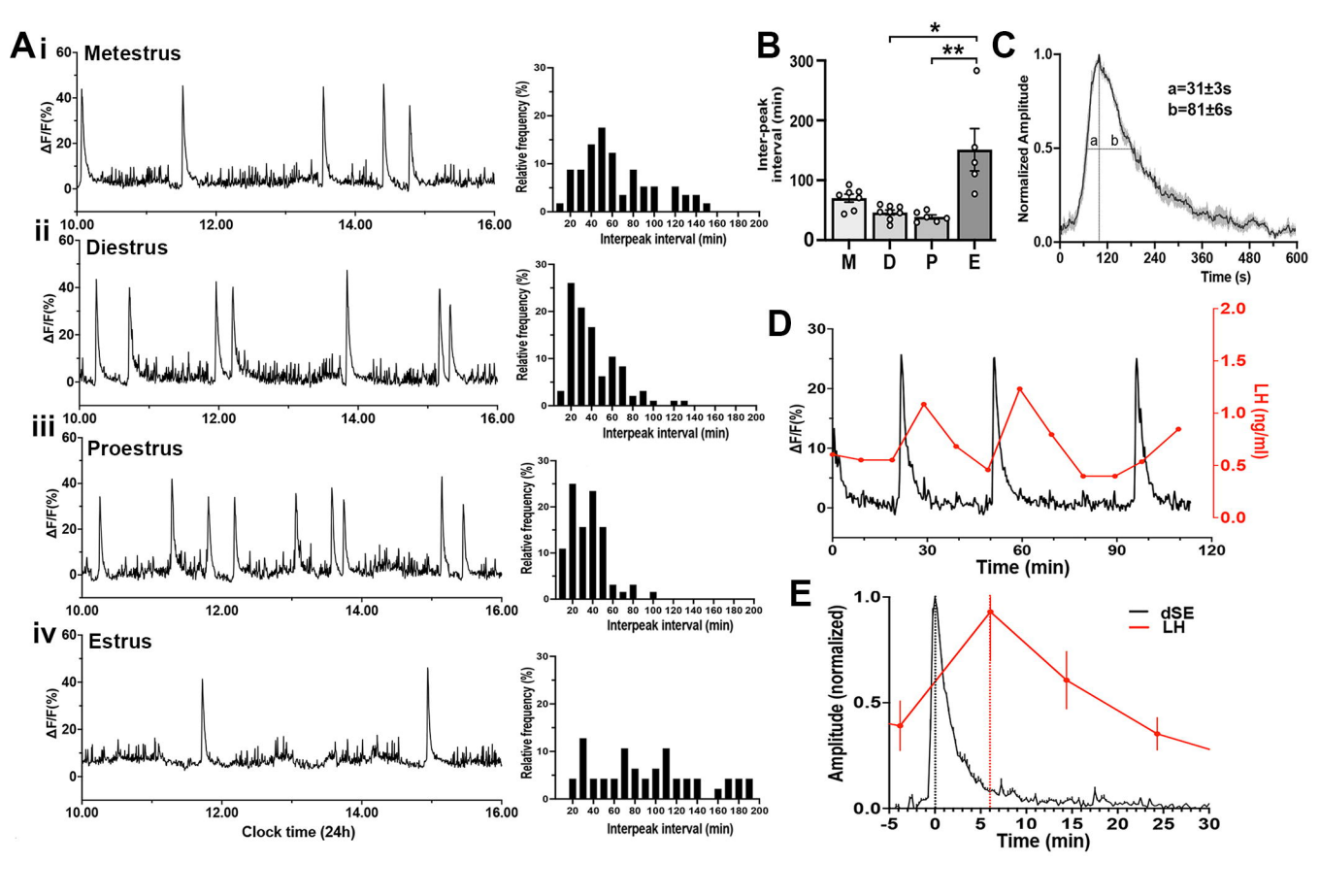
Ai
Metestrus
ii
Diestrus
iii
Proestrus
iv
Estrus
ΔF/F(%)
Clock time (24h)
Relative frequency (%)
Interpeak interval (min)
B
Inter-peak interval (min)
M
D
P
E
C
a=31±3s
b=81±6s
Normalized Amplitude
Time (s)
D
LH (ng/ml)
Time (min)
E
dSE
LH
Amplitude (normalized)
Time (min)

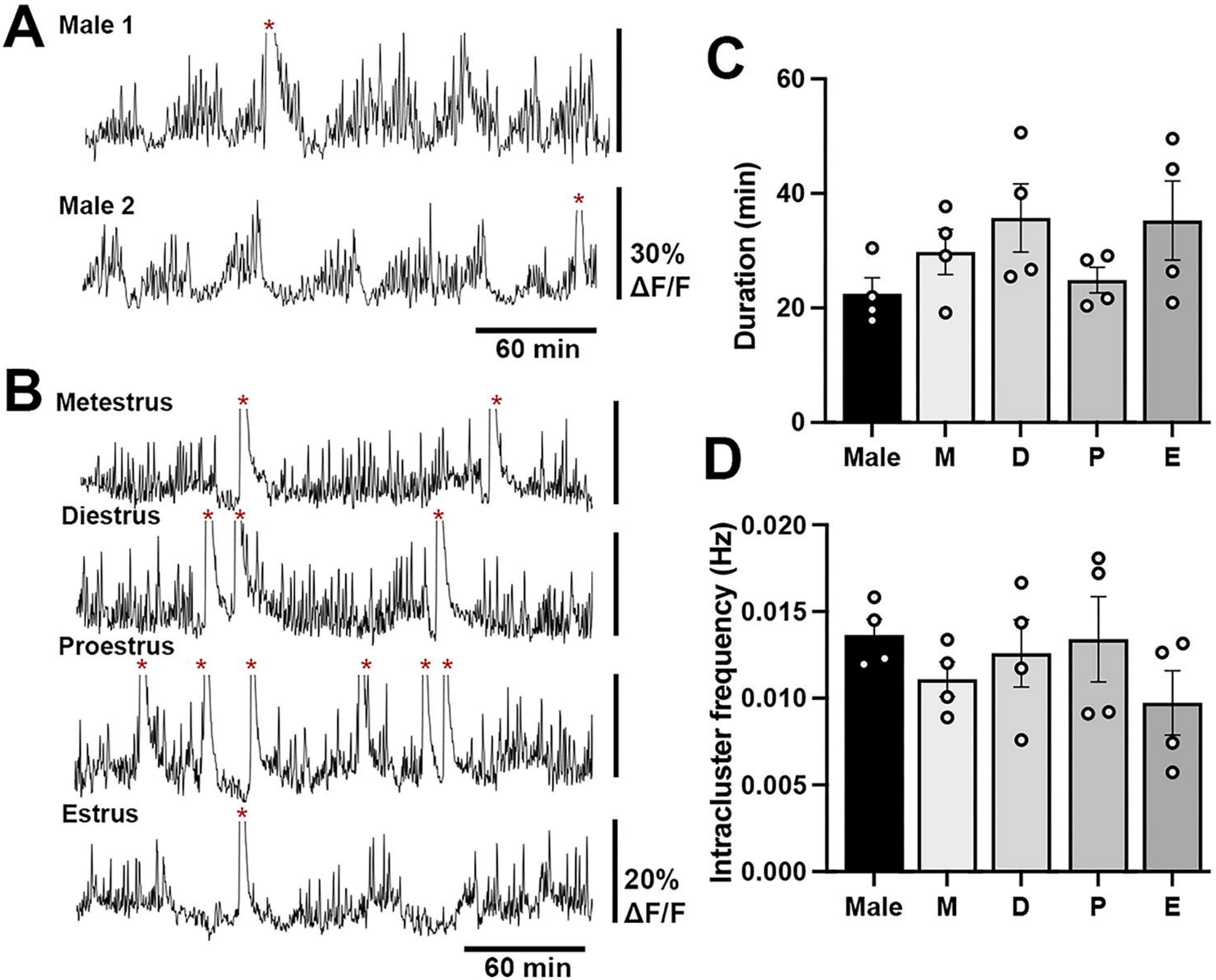
A
Male 1
Male 2
30%
ΔF/F
60 min
B
Metestrus
Diestrus
Proestrus
Estrus
20%
ΔF/F
60 min
C
Duration (min)
60
40
20
0
Male
M
D
P
E
D
Intracluster frequency (Hz)
0.020
0.015
0.010
0.005
0.000
Male
M
D
P
E

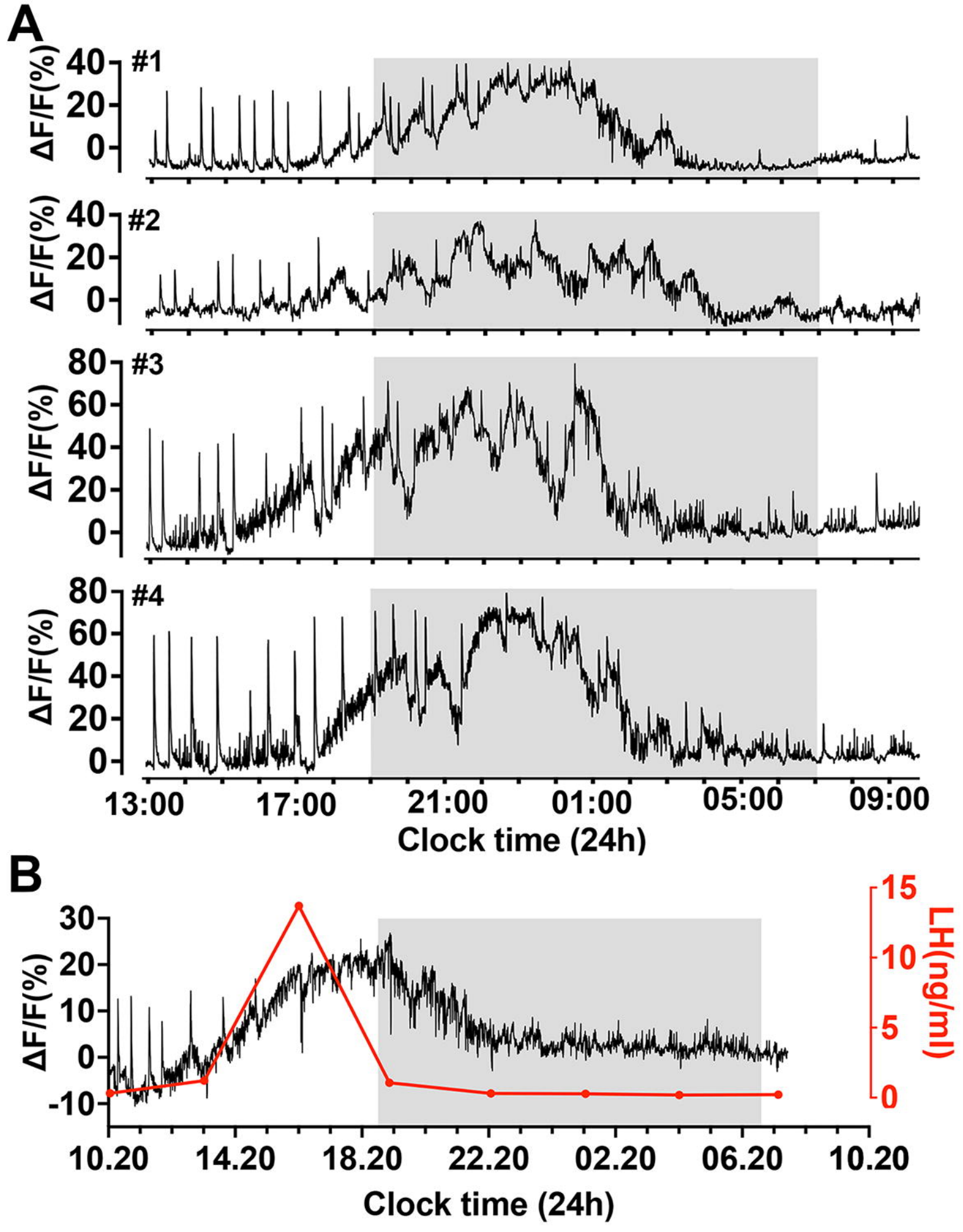
A
#1
#2
#3
#4
ΔF/F(%)
40
20
0
80
60
13:00
17:00
21:00
01:00
05:00
09:00
Clock time (24h)
B
30
10
-10
15
5
LH(ng/ml)
10.20
14.20
18.20
22.20
02.20
06.20
10.20
Clock time (24h)

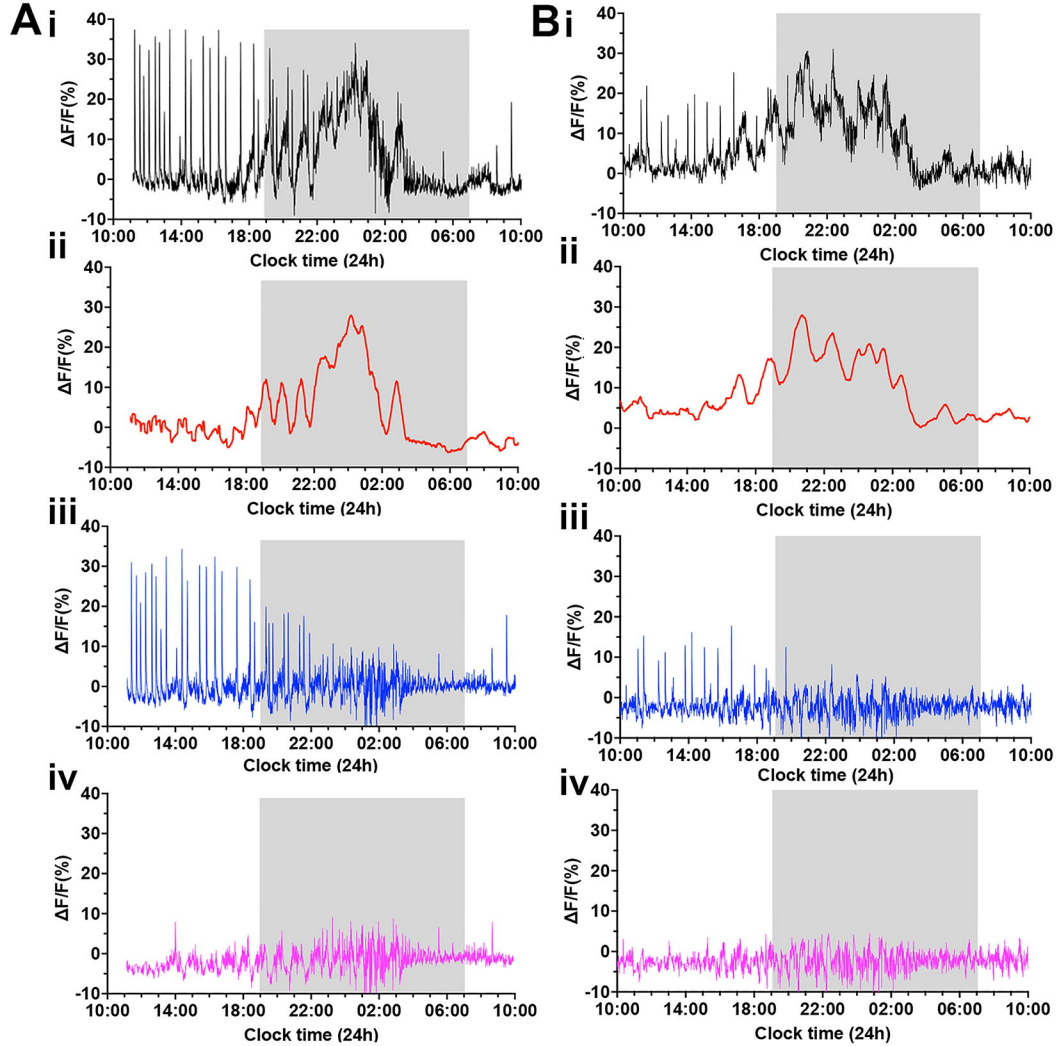
A i
ii
iii
iv
B i
ii
iii
iv
ΔF/F(%)
Clock time (24h)
10:00
14:00
18:00
22:00
02:00
06:00
10:00
40
30
20
10
0
-10